

HOW TO BUILD A 300 BIT, 1 GIGA-OPERATION QUANTUM COMPUTER

ANDREW M. STEANE

*Centre for Quantum Computation, Department of Atomic and Laser Physics,
Clarendon Laboratory, Parks Road, Oxford, OX1 3PU, England*

Received (received date)

Revised (revised date)

Experimental methods for laser control of trapped ions have reached sufficient maturity that it is possible to set out in detail a design for a large quantum computer based on such methods, without any major omissions or uncertainties. The main features of such a design are given, with a view to identifying areas for study. The machine is based on 13000 ions moved via $20\mu\text{m}$ vacuum channels around a chip containing 160000 electrodes and associated classical control circuits; 1000 laser beam pairs are used to manipulate the hyperfine states of the ions and drive fluorescence for readout. The computer could run a quantum algorithm requiring 10^9 logical operations on 300 logical qubits, with a physical gate rate of 1 MHz and a logical gate rate of 8 kHz, using methods for quantum gates that have already been experimentally implemented. Routes for faster operation are discussed.

Keywords: quantum computer architecture fault-tolerant

Communicated by:

The problem of making quantum computing feasible has been addressed from two main directions: the implementation of experimental methods to manipulate quantum systems, and the discovery of general methods to control errors and noise without destroying the coherence of a quantum computation. Several recent developments of experimental methods for laser-control of trapped ions have allowed a much greater degree of confidence that such methods can be extended to the sort of system size which would make a significant quantum computer (QC) [1, 2, 3, 4, 5, 6, 7, 8, 9]. Meanwhile, quantum error correction (QEC) circuits have been analyzed in sufficient detail to allow a discussion of the physical requirements of a large computer without any major omissions [10, 11]. By bringing these two aspects together, it is possible to outline one way to build a QC that is technologically feasible and does not require a very great degree of uncertainty in extrapolation from already established results. This article offers such an outline. Although we don't yet know if various details of the method described here are the best ones to use to build a large machine, it sets out the main issues and clarifies the vision for future work.

It is essential to the present argument that I only invoke micro-fabrication technology that is already available, time- and distance-scales close to those already explored in laboratory experiments, and techniques that have been demonstrated sufficiently to show all the ingredients required for repetitive QEC working together in a single experiment. Many different QC designs could be produced if one were to relax one or more of these requirements, but this would be a less valuable exercise because unexpected noise sources are always discovered

when experiments are done. The only assumptions I make are that established techniques can be implemented with more laser power and stability, in a parallelized form, and that the ion trap structures can be integrated with the necessary control circuitry.

The basic elements which would be required to make a general-purpose QC (qubits, gates and readout) were proposed by Deutsch [12]. Discussion of possible physical implementations has generated a large literature; most of the major considerations have been summarised by DiVincenzo [13]. The essential requirement is that the computer can implement fault-tolerant QEC on a useful number of qubits, because once it can do that then it can compute as well. In the network model of computation which we adopt here, for QEC the operation needed most frequently is to move quantum information from one place to another, the next most frequent is a logic gate such as controlled-not or controlled-phase between neighbouring qubits, and after that measurement of qubits and single-qubit rotations[11].

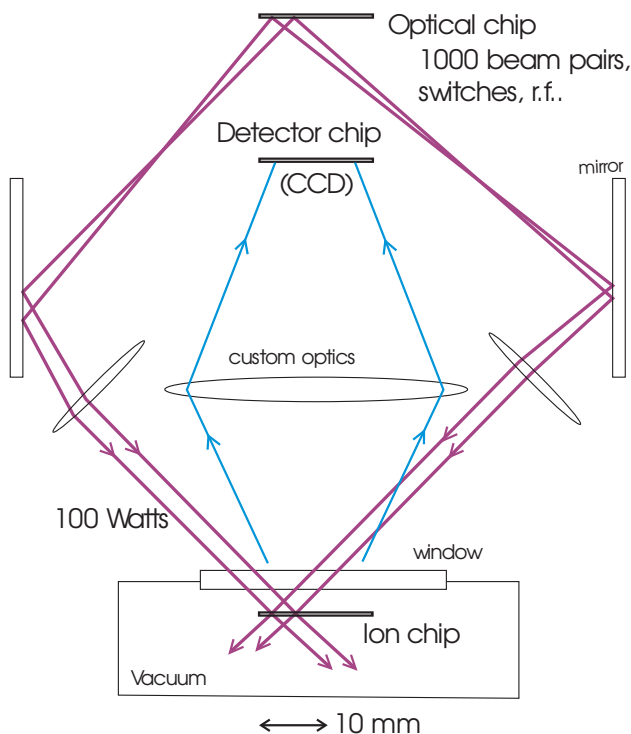


Fig. 1. Schematic diagram of the complete computer. An optical chip contains laser sources, optical switches and r.f. control circuitry for the laser pulses; the multiple laser beams (2 of 1000 pairs are shown) are imaged onto an 'ion chip' (IC) in vacuum, containing the array of ion traps and the control circuitry for moving ions around. The detector registers optical fluorescence; its elements could alternatively be incorporated onto the IC. The optical chip could alternatively be placed inside the vacuum chamber, close to the IC, or else replaced by conventional methods (stand-alone lasers, cavities and AOM's).

1 Overview

In this section the computer is described. The reasoning and technical arguments which lead to the choices of parameter values are given in section 2, and possibilities for improvements

are discussed in section 3.

A schematic diagram of the machine is shown in figure 1. The main parameters are defined below and listed in tables 1 and 2. Table 1 gives parameters of the overall design, such as the QEC encoding, the noise rates, the gate rate and the overall stability. Table 2 gives more detailed information on the physical processes and design.

Table 1. The main logical parameters of the computer. The parameters above the line describe the large-scale encoding. Those below the line use information from table 2 to provide the timing and noise parameters. The recovery ‘crash’ probability is the probability that recovery of a block fails, for example owing to an uncorrectable error, on the usual uncorrelated stochastic error model. Since this scales as γ_2^7 it is a very sensitive function of the noise level; the important point is that the error rates listed are low enough to allow a very large number of logical gates.

Encoding			
n. ion pairs (p-bits)	N		6444
block code parameters	$[[n, k, d]]$		[[127, 29, 15]]
ancilla circuit parameters	N_A, w		1939, 47
data+anc. bits per block	$4n + k$		537
n. blocks	$b = N/(4n + k)$		12
n. parallel operations	$N_P = 2bN_A/w$		990
n. parallel measurements	bn		1524
Overall performance			
physical gate time	$\tau_g = \frac{2}{\nu_{\text{sp1}}} + \frac{10}{\nu_r} + \tau_{\text{cool}} + \tau_p$		1.2 μs
syndrome processing time	t_{sp}		5 μs
logical gate rate	$1/(2w\tau_g + 2t_m + t_{\text{sp}})$		8 kHz
2-p-bit gate error	$\gamma_2 \simeq \epsilon_s + P_{\bar{n}}$		10^{-4}
1-p-bit gate error	γ_1		10^{-3}
measurement error	γ_m		10^{-3}
memory error	$\epsilon = 1/Q$		10^{-6}
recovery crash probability	$p \simeq$		10^{-10}
n. logical gates	$\simeq 1/(bp) \simeq$		10^9

The computer is made from two main elements: an array of linear r.f. Paul traps on an ‘ion chip’ (IC) held in high vacuum, with control circuitry for the trap electrodes integrated on the chip, and an optical system outside the vacuum chamber. The concept is broadly as proposed by Kielpinski et al. [14]. Qubits are stored in the hyperfine structure of ions; these are held in an array of ion traps on a chip in high vacuum, moved around by control voltages on the multiple electrodes, manipulated by coherently driven Raman transitions, and measured by laser-stimulated fluorescence. The IC contains 160,000 electrodes of dimensions of order 1 μm , individually controllable at switching rates of order 50 MHz and voltages of order 100 V by the classical control circuitry integrated on the IC.

The optical system must deliver 990 laser beam pairs to the IC, aligned to $\sim 1 \mu\text{m}$ with a power of 10 to 200 mW per beam (depending on the ion species and pointing stability). Each pair should have a precise frequency difference of order 10 GHz, or else the beams may each be frequency-modulated, depending on details of how the gates are implemented. This r.f. oscillation must be controlled by phase-locked high-quality circuitry similar to that used in nuclear magnetic resonance spectrometers, delivering pulses of duration 0.1 to 1 μs . The laser beams should be switched with very high extinction ratio on the same timescale.

Major savings in the construction scale and the power requirements would be made if the optical system could be integrated onto a second chip. This is an important aim for future technology, but even if it could not be done then one could still realise the optical system,

by duplicating current techniques such as solid-state lasers and acousto-optic modulators a thousand-fold. This is discussed further below.

For each QEC of the computer, around 1500 measurements are required at once, each involving 2 ions. Optical detection could be integrated onto either the IC or an optical chip, or else a separate detection chip is used, having at least 1500 pixels which can be read out individually in a time scale of order 1 μ s.

The large-scale parameter values, such as the total number of ions and laser beam pairs, are dictated by the requirement to perform QEC repetitively, and the decision of how large a machine to attempt. For the sake of having a concrete example that would comfortably out-perform any classical computer on suitably chosen algorithms, I choose the benchmark of 10^9 logical operations on 300 logical qubits. That is, the computer is designed to handle an algorithm of this size with a substantial probability of success.^a A single 300-qubit computer could not factorize numbers of interest to cryptography, but quantum algorithms to study eigenvalue problems, spin systems, and quantum chemistry are predicted to out-perform classical computers once 50 to 100 qubits are available[15, 16, 17].

Various types of QEC encoding are possible; in particular there is a trade-off between the noise level that can be tolerated and the number of physical qubits required [10, 18]. I choose to design for gate noise at the level 10^{-4} , and adopt the most efficient encoding that can achieve the required noise-tolerance. A more full statement of the error model is given in section 2. The result of these choices is a large block-code encoding using the $[[n, k, d]] = [[127, 29, 15]]$ CSS code based on a classical BCH code [19, 20, 10]. This performs very well under random errors. In order to enhance the robustness to an important type of systematic error, namely correlated phase error, such as is caused by joint energy level shifts of adjacent ions, or drift of a local oscillator phase, a low-level encoding using a two-qubit ‘decoherence free subspace’ is concatenated with the large code [21, 22, 23]. After the QEC is taken into account, I find a logical gate rate of approximately 10 kHz, limited by the physical gate rate, so that it would take about 30 hours to complete the $O(10^9)$ logic operations which are in principle available. This might appear ‘slow’ (though of course it still out-performs any classical computer on suitably chosen algorithms), but the logical gate rate of a QC will necessarily be slow compared to that of a good classical processor, first because the QC relies on very precise classical control circuitry, and secondly because a non-negligible amount of classical processing must take place in each logical step, in order to interpret the 78-bit syndromes of the BCH code. I have allowed 5 μ s for this classical processing. The reason for this choice is that it is long enough to appear reasonable, and short enough to have almost negligible impact on the logical gate rate for the computer under discussion. The main limits on speed come from the need to avoid photon scattering when the quantum gates are driven by optical pulses, and the time taken to move ions around the channels in the chip; I discuss faster operation below.

1.1 Feasibility

The IC has vacuum channels of width 20 μ m, electrodes of width around 1 μ m, voltages in the region 10 to 100 V, and an r.f. frequency for the Paul traps of 660 MHz. All these values are

^aAlgorithms, both classical and quantum, typically require many more gates than bits; these values would be appropriate if the number of gates scales as $40n^3$, for example.

close to those already implemented in single ion traps or ion trap arrays [24, 25, 3, 26, 27]. The major new ingredient is the large number of electrodes ($\sim 160,000$) and parallel operations (~ 1000 are required to allow fault-tolerant QEC at the assumed noise levels). This implies that a large amount of control circuitry must be integrated onto the IC because there is not room for sufficient wires to circuitry located elsewhere. Although this is a considerable design problem, the size and speed (switching times of order 10 ns) of these circuits are within the capability of current fabrication techniques. The substrate could for example be silicon.

The measurement and quantum gate techniques are precisely those already demonstrated in studies such as [1, 3, 2, 5, 6, 7, 8, 9]; I have merely picked some reasonable numbers for detection efficiency, and assumed sufficient laser power to enable the gate to be operated by a Raman process sufficiently far detuned that Raman scattering is below 10^{-4} per gate. I also assumed technical problems such as laser intensity noise and mechanical jitter on optical paths can be reduced sufficiently so that their contribution to errors per gate is below 10^{-4} . This would require the path difference of each Raman beam pair to be stable to \sim a few nm during τ_p (defined in table 2), but it can vary between gates by much larger amounts. Electrical noise, which may include cross-talk in the IC electronics, must be small enough to allow the ion locations to be similarly stable during the phase-gate time.

Placing the optical system outside the vacuum chamber would reduce several aspects of the fabrication problem. The high-quality imaging optics and interferometrically-stable mounting which are required to focus the laser beams onto the IC are not especially demanding compared to high-end optical instrumentation currently available. If each laser beam diameter at the IC is $4\ \mu\text{m}$ in order to make the required numerical aperture and alignment precision reasonably straightforward, then the total laser power required for ~ 1000 parallel operations is from some tens to several hundred Watts, depending on speed and, to a lesser extent, on ion species. It is important therefore to prevent these laser beams impinging on the IC. This is possible either with a planar design and laser beams propagating parallel to the IC surface, or by fabricating the IC with holes in it to allow the beams to pass through. These holes would only use up a small fraction of the chip area available for control circuitry. A smaller beam diameter might be preferred in order to reduce the power requirement. If instead the optical chip were inside the vacuum chamber, then the focussing elements would be integrated onto it and it would be close to the IC (e.g. a few mm away). This construction would exclude air pressure fluctuations and would allow higher rigidity, hence allowing smaller laser beam diameter and power.

Scattering during readout must also be avoided. The laser beams used for readout have intensity of order the saturation intensity I_0 , i.e. some 10^6 times smaller than the Raman beam pairs. A fluorescing ion emits a total power of order $\Gamma hc/2\lambda \simeq 10^{-10}W$, while each readout laser beam power is of order $\pi r^2 I_0 \simeq 1\ \mu\text{W}$. To make the scattered background considerably smaller than the fluorescence rate, we require less than 10^{-5} of the readout beam power to be scattered.

The total laser power required for the Raman beams is also feasible, though since laser sources are inefficient it would require careful power handling to extract heat. The major problem is to control 1000 laser beam pairs in high precision pulses of duration of order $1\ \mu\text{s}$. To produce the required pulses current experiments use acousto-optic and electro-optic modulators. These are of centimetre dimensions and dissipate 1 Watt of r.f. drive power

each. An array of thousands of such devices maintaining the required stability would be a formidable, though perhaps possible, engineering challenge. However, steering mirror arrays fabricated by MEMS can already achieve switching times of order $10 \mu\text{s}$, and sidebands can be impressed onto semiconductor diode laser output by low-power r.f. modulation of the drive current. It is reasonable to expect that these or related techniques will make the optical system feasible.

The physical gate rate is found to be of order 1 MHz, and this places the main limitation on the logical gate rate. However, given that the quantum gates rely on precise r.f. control pulses, it is important that we do not assume too fast an operation of the classical control circuitry, otherwise that would itself become the major constraint on feasibility.

2 Methods

The QC is designed to freely manipulate 290 logical qubits, and to do this it uses a further 58 logical qubits in two blocks as workspace in fault-tolerant logical operation circuits [28, 21, 29, 30, 31]. There are two layers of encoding: first each pair of physical qubits stores a single logical bit by the ‘decoherence free’ encoding $|0\rangle \rightarrow |01\rangle$, $|1\rangle \rightarrow |10\rangle$, which protects it from joint phase noise [21, 32, 23, 14]. For brevity I refer to these pair-encoded logical bits as ‘p-bits’. The p-bits are then encoded in a large block code, the $[[n, k, d]] = [[127, 29, 15]]$ CSS code based on a classical BCH code [19, 20, 10]. Each p-bit, or else a substantial fraction of the p-bits, is accompanied by a further ion of another species in order to allow sympathetic cooling.

Let the quantum memory quality factor Q be defined as the ratio of the decoherence time of a p-bit to the time required to complete a controlled operation on a pair of p-bits which were initially separated by a distance of order 10 p-bits. Let γ_2 be the imprecision (error probability) of a controlled phase gate between two p-bits which were initially separated by of order 10 p-bits. γ_1, γ_m are the error probability of a Hadamard (or equivalent) rotation of a single p-bit, and of a measurement of a p-bit, respectively. The reason to specify a distance of 10 p-bits comes from a study of typical distances in QEC recovery circuits [11], I will return to this point below.

The estimate in table 1 of the ‘crash’ probability p per recovery of one block is calculated using the formulae in [10]. The recovery networks have many more 2-bit gates (these can be controlled-not or controlled-phase) than 1-bit gates or measurements, therefore the errors γ_1, γ_m can be substantially larger than γ_2 without much effect on p .

To establish the speed of the computer, first consider measurement of physical qubits. A single recovery involves 2 measurements (1 to verify the ancilla, 1 to acquire the syndrome). Therefore twice the measurement time is a lower bound on the logical gate time, unless the computer size is increased in order to prepare further ancillas in the background so that they are ready when needed.

The hyperfine state of each ion is inferred from laser-stimulated fluorescence. I assume a detector counts photons, and I set a threshold of 2 counts, so that the measurement error is estimated in table 2 as the probability that a fluorescing ion only gives 0 or 1 counts. For this probability to fall below 10^{-3} we require the mean count to be 10 or more. A reasonable value for combined collection and detection efficiency is 0.02, and therefore^bthe measurement

^bThe excited fraction for a saturated ion is between 1/4 and 1/2, depending on the gross structure.

time is $t_m \simeq 2000/\Gamma \simeq 10 \mu\text{s}$.

Another basic time-scale is set by laser power constraints and the need to avoid photon scattering during physical gate operations. The 2-p-bit controlled gate can be achieved either by a controlled-phase gate between one ion from each pair, or by a joint gate on all four ions similar to that described in [14, 33]. The physics of the spin-flip and phase-flip gates described in [33, 1] respectively is similar. The former may be preferred if the qubit transition is first-order insensitive to magnetic field changes [34, 7]; the latter may be preferred otherwise. The physical mechanism of these and other gates for trapped ions have in common the use of laser-excitation of the motion, and the fact that approximately P_0/η photons are scattered per ion during the gate, where P_0 is the number which would be scattered during a π -pulse on the carrier (i.e. non motion-changing) excitation, and η is the Lamb-Dicke parameter. Decoherence of the hyperfine state is caused by Raman (not Rayleigh) scattering [35]. The total (Raman and Rayleigh) scattering also heats and decoheres the motion, which is important during a 2-qubit gate when the qubits and motion are entangled. To estimate the latter, note that one photon recoil $\hbar k$ at time t causes a change in coherent state parameter $\Delta\alpha = i\eta \exp(i2\pi\nu_{\text{str}}t)$. This changes the orbit area and hence accumulated phase by an amount of order η . After N_s scattering events at random times the resulting infidelity is of order $(N_s\eta^2/2)$. The total infidelity due to scattering, ϵ_s , is the sum of this and the half the number of Raman-scattering events during a gate^c. To obtain the latter, note that $\epsilon_s < 10^{-4}$ requires a detuning Δ from dipole-allowed transitions of the order of or larger than the fine structure. We first consider the local minimum in $P_0(\Delta)$ when the detuning is in between the fine structure components, near $\Delta = (\sqrt{2} - 1)\omega_F$, see [34]. At this detuning, the total scattering is dominated by Raman scattering, and for a ‘clock’ ($M = 0-0$) transition, assuming linear polarizations in order to reduce differential Stark shifts, the local minimum value is $P_0 \simeq 2\sqrt{2}\pi\Gamma/\omega_F$ per ion. This suggests that large fine structure splitting ω_F , and therefore a heavier ion, is advantageous. However, for $|\Delta| \gg \omega_F$ all the usual ions (groups IIA, IIB and Yb) can achieve low enough ϵ_s , so other considerations, such as required laser wavelength and power, and hyperfine repumping are more important. Let I_{P_0} be the laser intensity which would be required to obtain the desired gate rate when Δ is at the local minimum. Then at the actual operating point $|\Delta| > \omega_F$, the Raman scattering per gate is smaller than $2P_0/\eta$ by the ratio I_{P_0}/I where I is the laser intensity,^d while the total scattering per gate $N_s \simeq 2P_0/\eta$. Therefore the total infidelity due to photon scattering from both ions is $\epsilon_s \simeq (I_{P_0}/I + \eta^2)P_0/\eta$. In table 2 we specify the required ϵ_s and invert this into a formula for I .

By using well-chosen pulse design, the gate rate can approach and even exceed the vibrational frequency [36], but this exacerbates photon scattering. In order not to assume too great a reliance on advanced techniques, I take the inverse gate time $1/\tau_p$ to be of the order of the motional frequencies (centre of mass and stretch modes) of one pair of ions, $\tau_p = 4/\nu_{\text{str}}$. Usually $\eta P_0 \ll \epsilon_s$ so the η^2 (heating) term in ϵ_s can be dropped, and then

$$\tau_p \propto (I\lambda\epsilon_s/m)^{-1/2}. \quad (1)$$

^cThis assumes that population ‘leaking’ away by Raman scattering to hyperfine Zeeman sublevels outside the computational basis can be reclaimed at little cost, for example by optical pumping. This is non-trivial however and may favour ions with small F and large hyperfine splitting.

^dWe ignore other gross structure levels, which is valid as long as ϵ_s is not too small.

This formula summarises the way atomic parameters and available laser intensity constrain the gate time for a pair of neighbouring ions. To make this time contribute similarly to the measurement time for each logical gate, one would choose (see table 1) $\tau_p \simeq t_m/w \simeq 0.2 \mu\text{s}$. However, the laser power requirements are severe, and therefore I adopt here $\tau_p \simeq 0.5 \mu\text{s}$ in order to save power without much cost in overall speed (this gives $\eta = 0.07$ for Cd, $\eta = 0.06$ for Ca). With the further contribution of the time for moving ions around, this implies that the logical gate rate of this QC is limited by the physical gate rate, not the measurement time.

A complete gate operation between p-bits initially at different locations involves 5 steps: split, move, recombine, cool, operate. The ‘split’ is the process of pulling apart two ions which were close together (in order to separate one p-bit from another p-bit), ‘recombine’ is the reverse process. I allow a time of $2/\nu_{\text{spl}}$ for the split and recombine stages, where ν_{spl} is the centre of mass frequency of a pair of ions at the moment during the split when the potential barrier between them just appears, so that they are in a quartic rather than quadratic potential. This frequency can be made large by using large voltages on the electrodes, but there is a limit set by electrical breakdown. This is discussed in [27] and leads to the formula given in table 2 in terms of a geometric factor μ_8 and the maximum allowed electric field at the electrode surfaces E_{max} . Micro-fabricated ion trap structures of similar dimensions to those considered here have been found to operate at electric fields up to 10^9 V/m [37], which is the region where field emission can occur. To be cautious I take the maximum allowed d.c. electric field to be $2 \times 10^8 \text{ V/m}$. The split time scales almost linearly with the distance scale of the electrodes, parametrised by the nearest distance ρ from a trapped ion to an electrode surface. The value of ρ is limited by fabrication ease and by heating problems.

I model heating of trapped ions as due to electric field noise at the ions, in which case the heating rate is given by $d\bar{n}/dt = e^2 S(\nu)/4m\hbar\nu$ where \bar{n} is the mean vibrational quantum number and S is the spectral density of electric field fluctuations (dimensions $(\text{V/m})^2\text{Hz}^{-1}$). The results of a number of experimental studies of heating rates in small ion traps, summarised in [38], can be fitted by the empirical formula $S \simeq a/\rho^4$ where $a = 10^{-26\pm 1} (\text{Vm})^2\text{Hz}^{-1\epsilon}$. If we require that during the split time this heating results in $\Delta\bar{n} \leq 1$, then we obtain a lower bound $\rho \geq 5 \mu\text{m}$ when $\mu_8 E_{\text{max}} = 4 \times 10^6 \text{ V/m}$. This is for electrodes at room temperature; the heating could be reduced by cooling the electrodes.

A lower bound $\rho \gg \lambda$ applies to the gate zone (i.e. where quantum logic-gate laser pulses are applied), coming from the need to allow laser beams to be kept clear of the electrode structures. This also results in ρ of order microns.

Next, consider moving the ions once they have been split. Each p-bit pair is moved as a single entity. The required networks of operations are chiefly those which create and verify ancillas. It was shown in [11] that if the qubits are laid out along a line, then the mean separation of bits which must have a gate between them, averaged over all the gates in the network, is 22 bits. This gives the order of magnitude of the distance over which ions will have to be moved. It is advantageous to arrange the ions of each ancilla in a rectangular array rather than a line, which will reduce the average communication distance. I take the total movement time to be $10/\nu_r$ where ν_r is the radial confinement frequency calculated for

^eA model to explain the noise level and the ρ^4 dependance is put forward in [39], the large uncertainty in a is due to the fact that it may depend on surface quality and ion species as well as other factors.

a Paul trap having distance scale ρ , Mathieu q parameter 0.3 and maximum r.f. electric field 10^8 V/m, see table 2.

I adopt $\rho = 10 \mu\text{m}$ for splitting and transport regions of the chip in order to obtain a high speed while keeping the heating rate acceptably small, so that once ions arrive at a gate region they can be laser-cooled rapidly. To reduce heating of ions during the controlled logic-gate laser pulse where it would result in infidelity, the gate should be implemented in a zone slightly displaced from the splitting/recombining zone, with electrode surfaces further away by a factor 2 to 10.

The laser cooling requirement is set by the impact of non-zero temperature on gate fidelity. This was studied in [40] for a gate in the general class of those which are insensitive to thermal effects at first order in the Lamb-Dicke parameter, but sensitive to second order. The results give a reasonable guide for present purposes, where I assume that a gate in this class is to be implemented. It is found that to obtain an infidelity from thermal effects of 5×10^{-5} , it is sufficient to cool to a mean vibrational quantum number $\bar{n} = 0.5$ when $\eta = 0.07$. I assume that the motional heating which took place during the split and move only resulted in a few phonons' worth of heating. This and the fact that the required \bar{n} is not small compared to 1 allows the cooling time to be small, close to the inverse of the motional frequency.

I find that each of the 5 stages of a physical gate takes a similar time. The total time required is given in table 1, it is $1.2 \mu\text{s}$ for Cd, $1.08 \mu\text{s}$ for Ca.

This completes the discussion of the parameters giving the speed and noise tolerance of the computer. It remains to comment on the IC and optical sources.

The IC has of order 160,000 electrodes, allowing for 30 electrodes for each zone where gate operations take place, and a further 20 per p-bit for all the bits. Electrode voltage ramp times are of order 10 ns, with 990 separate zones of the IC to be activated in parallel. To allow on-chip logic and digital-to-analogue converters it is likely that silicon is the best substrate, though exploration of materials questions has only just begun. I assume that metal electrodes on a $\sim 10 \mu\text{m}$ thick layer of SiO_2 can be modelled roughly as capacitors with an r.f. loss tangent of order 0.0005. The distance scale ρ and the values given in table 2 for the radial confinement then imply the r.f. power dissipation is small (assuming ohmic heating in the conductors is negligible).

The laser beams used for gate operations are detuned by around the fine structure splitting, and this means that in order to obtain the desired gate speed they must be intense, with $I \simeq 18 \text{ mW}/\mu\text{m}^2$ for Cd^+ . To ease alignment the laser beam waists should not be too small. I allow a beam diameter $4 \mu\text{m}$. For Cd^+ this is 19λ , for Ca^+ it is 10λ , and therefore it is readily achievable in either case with high-quality optics. To reduce alignment errors and to prevent stray light from hitting electrodes it may be useful to use larger beams and pass them all through a reflective mask with $4 \mu\text{m}$ holes in it, which is then imaged onto the computer chip. In any case a uniformly illuminated $4 \mu\text{m}$ spot represents 220 mW per laser beam at the required intensity. This suggests the total laser power is $2 \times 0.22 \times 990 \simeq 440 \text{ W}$ for Cd^+ (100 W for Ca^+). In order to reduce the total instantaneous power one could separate in time the pulses on different ion pairs; this does not slow the computer when $\tau_p < \tau_g$.

3 Faster, larger, noisier

I conclude with a brief discussion of improvements and other approaches, towards faster operation and larger algorithm capability.

The logical gate rate could be increased without any change in the hardware apart from scaling up, by devoting more resources to preparing ancillas. There is up to a factor $\simeq 2w \simeq 100$ gain in speed available this way (i.e. until the recovery time is similar to the gate time), at a cost of the same factor increase in the number of ions, traps and laser beams.

Scaling up the number of physical bits, without a change in the number of logical bits, could instead be used to allow a higher noise threshold, by using a different QEC encoding. The threshold increases slowly with the computer size however; a very rough rule of thumb which summarises results in [10] is $N \propto \gamma^{2.5}$ for $\gamma < 0.003$ where γ is the physical gate error; higher noise is also possible with a similar cost [41, 18].

To reduce the measurement time some further ions could reside in each measurement zone on the chip, and when a given p-bit is to be measured, it is first coupled by controlled-not to these further ions and then all the ions in the set are simultaneously measured and a classical majority vote is taken to determine the result [42]. A speed-up is obtained as long as the controlled-not operations are fast compared to the measurement time.

To reduce the phase-gate and cooling time one could adopt fast pulse techniques as for example in [36], and increase the trap frequencies. This would require larger laser detuning and power to combat photon scattering. Once the measurement and phase gate time is reduced, it becomes worthwhile to use smaller electrode distance ρ in order to reduce the split and move time.

These improvements could gain several orders of magnitude in speed, or they could be used to make the machine more robust and therefore relax the engineering requirements. To further increase the gate rate it would ultimately be necessary to abandon optical methods to control and measure the ions, and adopt electronic methods instead. For example, one might transfer quantum information directly between an ion and an electron in a closely situated electrode [43]. However, one would then lose some very attractive features of optical control, and the electrons would be subject to a much larger and more complex set of processes which lead to decoherence than the quasi-free ions. The advantages of optical methods are chiefly that photons do not directly influence one another, they are insensitive to electromagnetic field noise, and their excitation energies are far above the thermal energy at room temperature, so they can be switched off completely.

Acknowledgements

This work was supported by the European Union through the IST/FET/QIPC project “QGATES” and by the National Security Agency (NSA) and Advanced Research and Development Activity (ARDA) (P-43513-PH-QCO-02107-1).

1. D. Leibfried, B. DeMarco, V. Meyer, D. Lucas, M. Barrett, J. Britton, W. M. Itano, B. Jelenkovic, C. Langer, T. Rosenband, and D. J. Wineland. Experimental demonstration of a robust, high-fidelity geometric two ion-qubit phase gate. *Nature*, 422:412–415, 2003.
2. M. Riebe, H. Häffner, C. F. Roos, W. Hänsel, J. Benhelm, G. P. T. Lancaster, T. W. Körber, C. Becher, F. Schmidt-Kaler, D. F. V. James, and R. Blatt. Deterministic quantum teleportation with atoms. *Nature*, 429:734–737, 2004.

3. M. D. Barrett, J. Chiaverini, T. Schaetz, J. Britton, W. M. Itano, J. D. Jost, E. Knill, C. Langer, D. Leibfried, R. Ozeri, and D. J. Wineland. Deterministic quantum teleportation of atomic qubits. *Nature*, 429:737–739, 2004.
4. J. Ignacio Cirac and Peter Zoller. New frontiers in quantum information with atoms and ions. *Physics Today*, 57(3):38–44, 2004.
5. K.-A. Brickman, P. C. Haljan, P. J. Lee, M. Acton, L. Deslauriers, and C. Monroe. Implementation of Grover’s quantum search algorithm in a scalable system. *Phys. Rev. A*, 72:050306(R), 2005.
6. H. Häffner, W. Hänsel, C. F. Roos, J. Benhelm, D. Chek-al-kar, M. Chwalla, T. Körber, U. D. Rapol, M. Riebe, P. O. Schmidt, C. Becher, O. Gühne, W. Dür, and R. Blatt. Scalable multiparticle entanglement of trapped ions. *Nature*, 438:643, 2005.
7. P. C. Haljan, P. J. Lee, K.-A. Brickman, M. Acton, L. Deslauriers, and C. Monroe. Entanglement of trapped-ion clock states. *Phys. Rev. A*, 72:062316, 2005. quant-ph/0508123.
8. D. Leibfried, E. Knill, S. Seidelin, J. Britton, R. B. Blakestad, J. Chiaverini, D. B. Hume, W. M. Itano, J. D. Jost, C. Langer, R. Ozeri, R. Reichle, and D. J. Wineland. Creation of a six-atom ‘Schrödinger cat’ state. *Nature*, 438:639–642, 2005.
9. J. Chiaverini, D. Leibfried, T. Schaetz, M. D. Barrett, R. B. Blakestad, J. Britton, W.M. Itano, J.D. Jost, E. Knill, C. Langer, R. Ozeri, and D.J. Wineland. Realization of quantum error correction. *Nature*, 432:602–605, 2004.
10. Andrew M. Steane. Overhead and noise threshold of fault-tolerant quantum error correction. *Phys. Rev. A*, 68:042322, 2003.
11. A. M. Steane. Quantum computer architecture for fast entropy extraction. *Quant. Inf. and Comp.*, 2:297–306, 2002. quant-ph/0203047.
12. D. Deutsch. Quantum theory, the Church-Turing principle and the universal quantum computer. *Proc. R. Soc. Lond. A*, 400:97–117, 1985.
13. D. P. DiVincenzo. The physical implementation of quantum computation. *Fortschritte der Physik*, 48:771–783, 2000.
14. D. Kielpinski, C. Monroe, and D. Wineland. Architecture for a large-scale ion-trap quantum computer. *Nature*, 417:709–711, 2002.
15. Daniel S. Abrams and Seth Lloyd. Quantum algorithm providing exponential speed increase for finding eigenvalues and eigenvectors. *Phys. Rev. Lett.*, 83:5162–5165, 1999.
16. D. Porras and J.I. Cirac. Effective quantum spin systems with trapped ions. *Phys. Rev. Lett.*, 92:207901, 2004.
17. Alán Aspuru-Guzik, Anthony D. Dutoi, Peter J. Love, and Martin Head-Gordon. Simulated quantum computation of molecular energies. *Science*, 309:1704–1707, 2005.
18. E. Knill. Fault-tolerant postselected quantum computation: Threshold analysis. 2004. quant-ph/0404104.
19. A. R. Calderbank and P. W. Shor. Good quantum error-correcting codes exist. *Phys. Rev. A*, 54:1098–1105, 1996.
20. A. M. Steane. Multiple particle interference and quantum error correction. *Proc. Roy. Soc. Lond. A*, 452:2551–2577, 1996.
21. Michael A. Nielsen and Isaac L. Chuang. *Quantum Computation and Quantum Information*. Cambridge University Press, Cambridge, 2000.
22. Christian F. Roos, Mark Riebe, Hartmut Häffner, Wolfgang Hänsel, Jan Benhelm, Gavin P. T. Lancaster, Christoph Becher, Ferdinand Schmidt-Kaler, and Rainer Blatt. Control and measurement of three-qubit entangled states. *Science*, 304:1478–1480, 2004.
23. D. Kielpinski, V. Meyer, M. A. Rowe, C. A. Sackett, W. M. Itano, C. Monroe, and D. J. Wineland. A decoherence-free quantum memory using trapped ions. *Science*, 291:1013–1015, 2001.
24. S.R. Jefferts, C. Monroe, E.W. Bell, and D.J. Wineland. A coaxial-resonator driven rf (Paul) ion trap for strong confinement. *Phys. Rev. A*, 51:1235, 1995.
25. M. G. Blain, L. S. Riter, D. Cruz, D. E. Austin, G. Wu, W. R. Plass, and R. G. Cooks. Towards the hand-held mass spectrometer design considerations, simulation, and fabrication of micrometer-scaled cylindrical ion traps. *Int. J. Mass Spectrometry*, 236:91–104, 2004.

26. M. J. Madsen, W. K. Hensinger, D. Stick, J. A. Rabchuk, and C. Monroe. Planar ion trap geometry for microfabrication. *Appl. Phys. B*, 78:639–651, 2004.
27. J. P. Home and A. M. Steane. Electrode configurations for fast separation of trapped ions. *Quant. Inf. Comp.*, 6:289–325, 2006. quant-ph/0411102.
28. P. W. Shor. Fault-tolerant quantum computation. In *Proc. 35th Annual Symposium on Fundamentals of Computer Science*, pages 56–65, Los Alamitos, 1996. IEEE Press. quant-ph/9605011.
29. D. Gottesman. A theory of fault-tolerant quantum computation. *Physical Review A*, 57:127–137, 1998. quant-ph/9702029.
30. D. Gottesman and I. L. Chuang. Quantum teleportation is a universal computational primitive. *Nature*, 402:390, 1999. quant-ph/9908010.
31. Andrew M. Steane and Ben Ibinson. Fault-tolerant logical gate networks for Calderbank-Shor-Steane codes. *Phys. Rev. A*, 72:052335, 2005. quant-ph/0311014.
32. C. F. Roos, G. P. T. Lancaster, M. Riebe, H. Häffner, W. Hänsel, S. Gulde, C. Becher, J. Eschner, F. Schmidt-Kaler, and R. Blatt. Bell states of atoms with ultralong lifetimes and their tomographic state analysis. *Phys. Rev. Lett.*, 92:220402, 2004. ion trap.
33. A. Sørensen and K. Mølmer. Quantum computation with ions in thermal motion. *Phys. Rev. Lett.*, 82:1971–1974, 1999.
34. D. J. Wineland, M. Barrett, J. Britton, J. Chiaverini, B. DeMarco, W. M. Itano, B. Jelenkovic, C. Langer, D. Leibfried, V. Meyer, T. Rosenband, and T. Schätz. Quantum information processing with trapped ions. *Phil. Trans. R. Soc. Lond. A*, 361:1349–1361, 2003.
35. R. Ozeri, C. Langer, J. D. Jost, B. DeMarco, A. Ben-Kish, B. R. Blakestad, J. Britton, J. Chiaverini, W. M. Itano, D. B. Hume, D. Leibfried, T. Rosenband, P. O. Schmidt, and D. J. Wineland. Hyperfine coherence in the presence of spontaneous photon scattering. *Phys. Rev. Lett.*, 95:030403, 2005.
36. J. J. Garcia-Ripoll, P. Zoller, and J. I. Cirac. Speed optimized two-qubit gates with laser coherent control techniques for ion trap quantum computing. *Phys. Rev. Lett.*, 91:157901, 2003.
37. D. Cruz, J. P. Chang, and M. G. Blain. Field emission characteristics of a tungsten micro-electrical mechanical system device. *Appl. Phys. Lett.*, 86:153502, 2004.
38. L. Deslauriers, P. C. Haljan, P. J. Lee, K.-A. Brickman, B. B. Blinov, M. J. Madsen, and C. Monroe. Zero-point cooling and low heating of trapped Cd ions. *Phys. Rev. A*, 2004. quant-ph/0404142.
39. Q. A. Turchette, D. Kielpinski, B. E. King, D. Leibfried, D. M. Meekhof, C. J. Myatt, M. A. Rowe, C. A. Sackett, C. S. Wood, W. M. Itano, C. Monroe, and D. J. Wineland. Heating of trapped ions from the quantum ground state. *Phys. Rev. A*, 61(6):063418, May 2000.
40. A. Sørensen and K. Mølmer. Entanglement and quantum computation with ions in thermal motion. *Phys. Rev. A*, 62:022311, 2000. quant-ph/0002024.
41. B. W. Reichardt. Improved ancilla preparation scheme increases fault-tolerant threshold. 2004. quant-ph/0406025.
42. David Stevens, Jerome Brochard, and Andrew Steane. Simple experimental methods for trapped-ion quantum processors. *Phys. Rev. A*, 58(4):2750–2759, 1998.
43. L. Tian, P. Rabl, R. Blatt, and P. Zoller. Interfacing quantum-optical and solid-state qubits. *Phys. Rev. Lett.*, 92:247902, 2004.

Table 2. Physical parameters of the computer. The list is in the order of the argument presented in the text. The bold parameters are the main ones used in table 1. The example values are given for the Cd^+ ion. Parameters for Ca^+ at the same gate rate give smaller laser power and a more convenient wavelength, but a more difficult hyperfine repumping.

Optical		
linewidth	Γ	$2\pi \times 44$ MHz
collection efficiency	ε	0.02
mean counts per ion	\bar{c}	10
P(0 or 1 count)	$(1 + \bar{c})e^{-\bar{c}}$	0.0005
measurement time	$t_m = 4\bar{c}/\varepsilon\Gamma$	7.2 μs
wavelength	λ	214 nm
saturation intensity	$I_0 = 4\pi^2\Gamma\hbar c/3\lambda^3$	11700 Wm^{-2}
mass number	$A = m/u$	111
recoil frequency	$R = h/2Au\lambda^2$	39 kHz
fine structure	ω_F	$2\pi \times 74$ THz
scattered photons at local minimum	$P_0 \simeq 2\sqrt{2}\pi\Gamma/\omega_F$	5.3×10^{-6}
infidelity from photon scattering	ϵ_s	4×10^{-5}
phase-gate time		
stretch mode frequency	$\nu_{\text{str}} \simeq 4/\tau_p$	8 MHz
c.o.m. mode frequency	$\nu_{\text{com}} = \nu_{\text{str}}/\sqrt{3}$	4.6 MHz
stretch-mode Lamb Dicke param.	$\eta = \sqrt{R/\nu_{\text{str}}}$	0.07
carrier Raman Rabi frequency	$\Omega_R = \pi/\eta\tau_p$	$2\pi \times 14$ MHz
laser intensity for P_0	$I_{P0} = 6\omega_F(3\sqrt{2} - 4)\Omega_R I_0/\Gamma^2$	9.2 $\text{mW}/\mu\text{m}^2$
intensity per laser beam	$I = I_{P0}P_0/(\eta\epsilon_s - \eta^2P_0)$	18 $\text{mW}/\mu\text{m}^2$
beam diameter	$2r$	4 μm
power per beam	$\pi r^2 I$	220 mW
total laser power	$2N_P\pi r^2 I$	440 W
Trapping: axial (d.c.)		
nearest distance to electrode	ρ	10 μm
d.c. electric field at electrode	E_{max}	200 $\text{V}/\mu\text{m}$
octopole geometric factor	μ_8	0.02
c.o.m. frequency at split	$\nu_{\text{spl}} = \frac{840}{2\pi\sqrt{A}} \left(\frac{\mu_8 E_{\text{max}}}{\rho^3} \right)^{3/10}$	15 MHz
Trapping: radial (r.f.)		
Mathieu q -parameter	q_r	0.3
r.f. quadrupole geometric factor	μ_4	0.15
r.f. electric field amplitude	E_{rf}	100 $\text{V}/\mu\text{m}$
r.m.s. voltage	$V_{\text{rms}} = \mu_4 \rho E_{\text{rf}}/\sqrt{2}$	106 V
radial secular freq.	$\nu_r = \frac{1}{2\pi} \left(\frac{q_r e}{2Au} \frac{\mu_4 E_{\text{rf}}}{\rho} \right)^{1/2}$	70 MHz
r.f. frequency	$\Omega/2\pi = 2\sqrt{2}\nu_r/q_r$	660 MHz
Electrical architecture		
total area	$50N\rho^2$	0.3 cm^2
n. d.c. electrodes	$30N_P + 20N$	160,000
electrode density		490,000 cm^{-2}
capacitance per p-bit	$C = 20\rho\epsilon_0$	0.002 pF
loss tangent	$\tan \delta$	0.0005
total r.f. power dissipated	$NV_{\text{rms}}^2\Omega C \tan \delta$	24 mW
Thermal		
mean vibration number	\bar{n}	0.5
Lamb Dicke gate error	$P_{\bar{n}} = 0.3\pi^2\eta^4\bar{n}(\bar{n} + 1)$	5×10^{-5}
cooling time	$\tau_{\text{cool}} = 1/\bar{n}\nu_{\text{com}}$	0.4 μs
heating rate in gate zone	$d\bar{n}/dt$	1 ms^{-1}
heating during phase gate	$\Delta\bar{n} = \tau_p d\bar{n}/dt$	~ 0.0005